

Electronic Supplementary Information

Stable and efficient colour enrichment powders of nonpolar nanocrystals in LiCl

Talha Erdem,^{a,†} Zeliha Soran-Erdem,^{a,†} Vijay Kumar Sharma,^b Yusuf Kelestemur,^a Marcus Adam,^c Nikolai Gaponik^c and Hilmi Volkan Demir^{a,b,*}

^a*Departments of Electrical and Electronics Engineering, Physics, UNAM–National Nanotechnology Research Center, and Institute of Materials Science and Nanotechnology, Bilkent University, 06800, Turkey.*

^b*School of Electrical and Electronic Engineering and School of Physical and Mathematical Sciences, Nanyang Technological University, 639798, Singapore.*

^c*Physical Chemistry, TU Dresden, Bergstrasse 66b, D-01062 Dresden, Germany.*

Author Contributions

[†] These authors contributed equally to this paper.

Corresponding Authors

*E-mail: volkan@bilkent.edu.tr and hvdemir@ntu.edu.sg

Characterizations

Scanning electron microscopy (SEM): The LiCl and NC-in-LiCl powders were imaged employing an FEI Quanta 200 FEG SEM. Samples were prepared by placing approximately 2 mg of only LiCl and NC embedded LiCl powders onto a carbon tape. Following 4 nm of Au/Pd coating, the samples were imaged under high vacuum.

Transmission electron microscopy (TEM): The TEM images of the green-emitting CdSe/CdZnSeS/ZnS nanocrystals and NC embedded LiCl powders were taken using a FEI Tecnai G2 F30 transmission electron microscope. For this purpose, TEM sample of NCs and NC embedded LiCl powders were prepared by drop-casting of diluted NC dispersion in hexane and powder dispersion in pure ethanol on a 200 mesh copper grid, respectively.

Fourier transform infrared spectroscopy (FT-IR): Chemical differences of the NCs with and without LiCl encapsulation were investigated using a Shimadzu DR-8101 Fourier transform infrared spectrometer. The sample of the NCs without LiCl encapsulation was prepared by drop-casting 50 μ L of the NC dispersion on a KBr pellet. The KBr pellets of only LiCl and NC incorporated LiCl powders were prepared by mixing 7.5 mg of the

powders with 111.8 mg of KBr powder. Spectra of pellets were recorded between the wavelengths of 400-4000 cm^{-1} .

Thermal gravimetric analyses (TGA): TGA was performed using a TA Instruments TGA Q500 thermal gravimetric analysis tool. We performed TGA on the samples of only NC, only LiCl, and NC-in-LiCl powders. In addition, we drop-casted NCs in hexane on only LiCl powders and physically mixed the NCs with LiCl powders after evaporation of hexane. Prior to measurement, LiCl including samples were warmed to 100 °C under a nitrogen atmosphere, held at 100 °C for 15 min to discard the moisture and cooled to room temperature (RT). After 15 min waiting at RT, the temperature was ramped up to 980 °C at the heating rate of 10°C min^{-1} . Different than powders, only NC sample was heated directly to 980 °C with the same heating parameters. All measurements were performed under inert nitrogen environment.

X-ray photoelectron spectroscopy (XPS): XPS measurements were performed using a Thermo K-Alpha XPS spectrometer by referencing it to C 1s peak at ~285 eV. The spectra corresponding to Zn, Cd, Cl, Li, Se, and S were recorded.

Optimization of NC amount in macrocrystals

The optimization study of the NC incorporation amount in the LiCl ionic salt was carried out by integrating 0.3 (Sample 1), 0.4 (Sample 2), and 0.6 mg (Sample 3) of the NCs-in-LiCl. The photoluminescence spectra of these NC-in-LiCl powders were given in Figure S1. Their quantum efficiencies were measured as described in the Experimental Methods section to be 65.7%, 75.1%, and 72.5%. In the rest of the study, the samples were prepared by incorporating NCs having this highest quantum efficiency were employed.

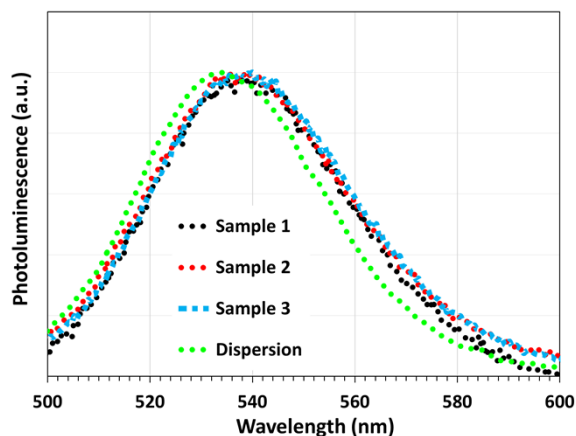


Figure S1. Photoluminescence spectra of the NCs in the dispersion and that of the same NCs-in-LiCl prepared using 0.3, 0.4, and 0.5 mg (Sample 1, Sample 2, and Sample 3) of the NCs.

Calculation of the NC molar concentration in LiCl powders

Because in this study we use the alloyed CdSe/CdZnSeS/ZnS NCs, whose exact composition cannot be known, exact determination of the molar concentration is not possible. However, an estimation of this concentration is still possible based on the size of the NCs and the density of the materials constituting the NCs (ignoring the contribution from ligands). We start our calculations with the assumption of spherical nanocrystals having a diameter of ca. 8 nm as determined from the TEM images. This leads to the volume of each individual NC to be $268.1 \times 10^{-21} \text{ cm}^3$. If the NCs were totally composed of CdSe, then their molecular weights would be $9.39 \times 10^8 \text{ mg/mol}$. If the material were CdS and ZnSe, then the molecular weights of the NCs would be $7.79 \times 10^8 \text{ mg/mol}$ and $8.51 \times 10^8 \text{ mg/mol}$, respectively. If the NCs were made of ZnS, then the corresponding molecular weights turn out to be $6.60 \times 10^8 \text{ mg/mol}$. Because the maximum and minimum molecular weights were obtained for CdSe and ZnS cases, the correct molecular weight should be between these two cases. Since we know the weight of the NCs inside 1 mg of the NC-in-LiCl powders to be 0.0122 mg, then the amount of the NCs inside 1 mg of powder turns out to be $\sim 13.0 \text{ pmol}$ for CdSe assumption and $\sim 18.4 \text{ pmol}$ for ZnS assumption.

SEM and TEM images

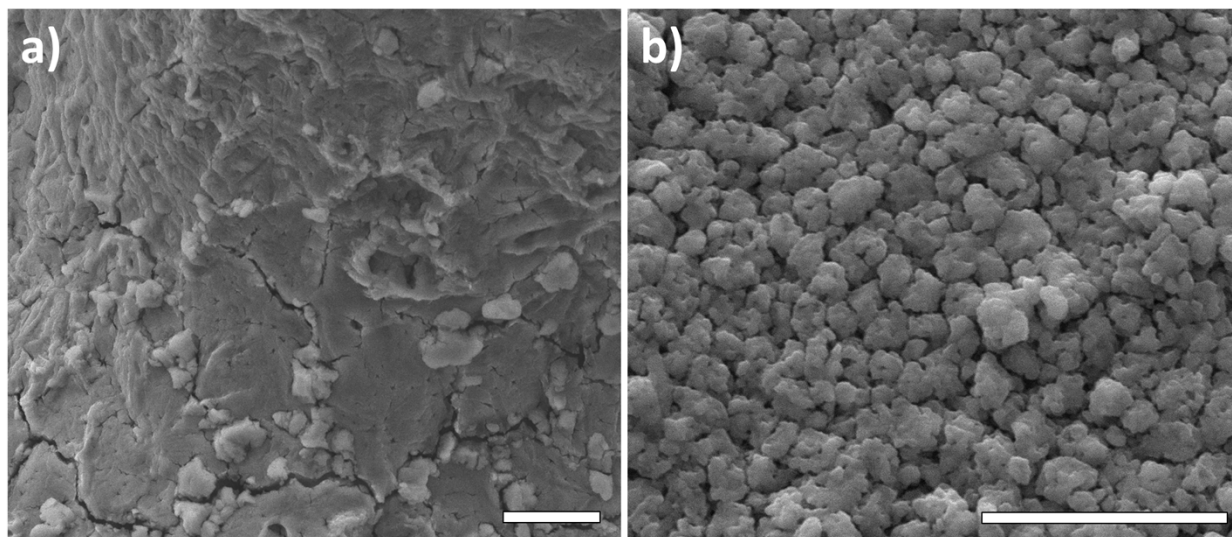


Figure S2. SEM images of (a) the only LiCl powder and (b) NC-in-LiCl powder. Scale bars: 10 μm .

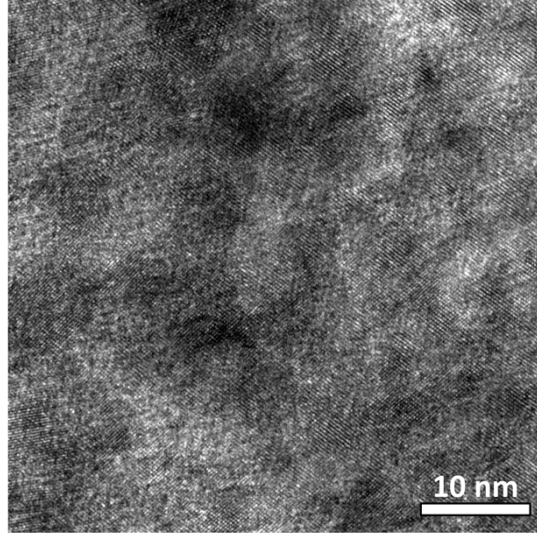


Figure S3. TEM image of the NCs within LiCl host.

The dependence of the radiative lifetime on the refractive index

According to Nienhuis et al.¹, the radiative lifetime is related to the refractive index in the absence of local-field effects as $\tau_{rad} = \frac{\tau_{vac}}{n}$ where τ_{rad} is the radiative lifetime in the dielectric medium, τ_{vac} is the radiative lifetime in the vacuum, and n is the refractive index.

When the dipole is placed in an empty spherical cavity, the radiative lifetime becomes

$$\tau_{rad} = \left(\frac{3n^2}{2n^2 + 1} \right)^{-2} \frac{\tau_{vac}}{n} \text{ according to Glauber et al.}^2 \text{ This model is called the empty-cavity model.}$$

When the dipole is placed within a cavity with the same refractive index as the host and the dipoles in the cavity do not contribute to the local electric field, the radiative lifetime becomes

$$\tau_{rad} = \left(\frac{n^2 + 2}{3} \right)^{-2} \frac{\tau_{vac}}{n} \text{ according to Knoester et al.}^3 \text{ This model is called the virtual-cavity model.}$$

Finally, Crenshaw et al.⁴ showed that the radiative lifetime becomes $\tau_{rad} = \left(\frac{n^2 + 2}{3} \right)^{-1} \tau_{vac}$ if the microscopic local-field effects were introduced. This model is called the fully microscopic model.

In our calculations, we first determined the vacuum radiative lifetime of the NCs using the radiative lifetime information of the NC dispersion. Subsequently, we predicted the radiative lifetime of these NCs according to these models as if they were surrounded by LiCl, and compared these results with the measured radiative lifetimes of NC-in-LiCl powders.

FTIR spectrum of the NCs and NC-in-LiCl powders

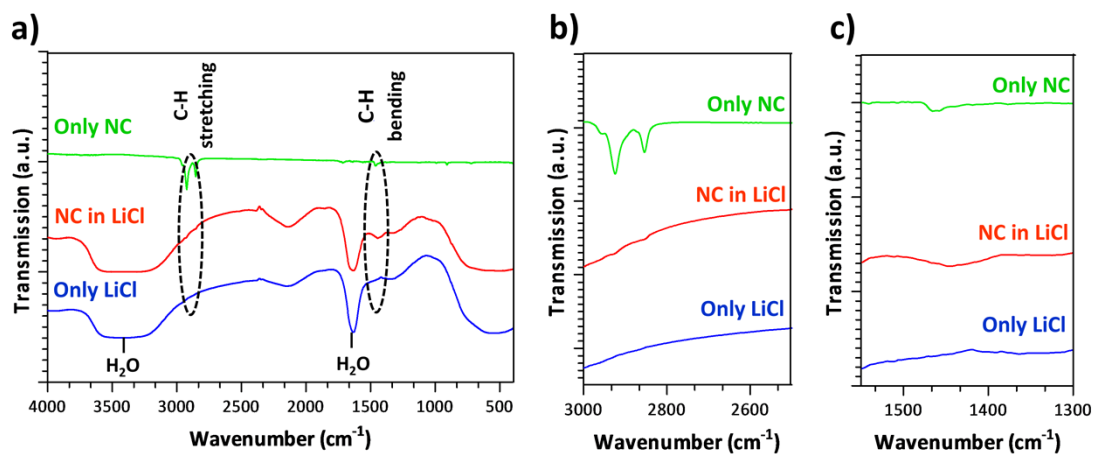


Figure S4. (a) FTIR spectra of the samples of only NCs along with LiCl powders with and without NC incorporation. The zoomed version of the same spectra between the wavenumbers of (b) 2500-3000 cm^{-1} and (c) 1300-1550 cm^{-1} .

The results presented in Figure S3 show that the FTIR spectrum of the only LiCl is coherent with the literature⁵. In FT-IR spectra of only NCs, which have oleic acid ligands, we observe strong C-H stretching bond around 2860-2924 cm^{-1} and C-H bending bond around 1450-1460 cm^{-1} belonging to the ligands of NC. Although both of the C-H bending and C-H stretching bonds are visible in NC embedded LiCl samples as well, their intensities are dominated. On the other hand, we expect to observe strong stretching bond belonging to C-Cl around 550-800 cm^{-1} if there were a chemical reaction between the NC ligand and LiCl. However, we could not see any peak around these wavenumbers. This suggests that LiCl only wraps the NCs without having a C-Cl bonding.

TGA measurements of the NCs, NC-in-LiCl powders, only LiCl powders, and NC drop-casted LiCl powders

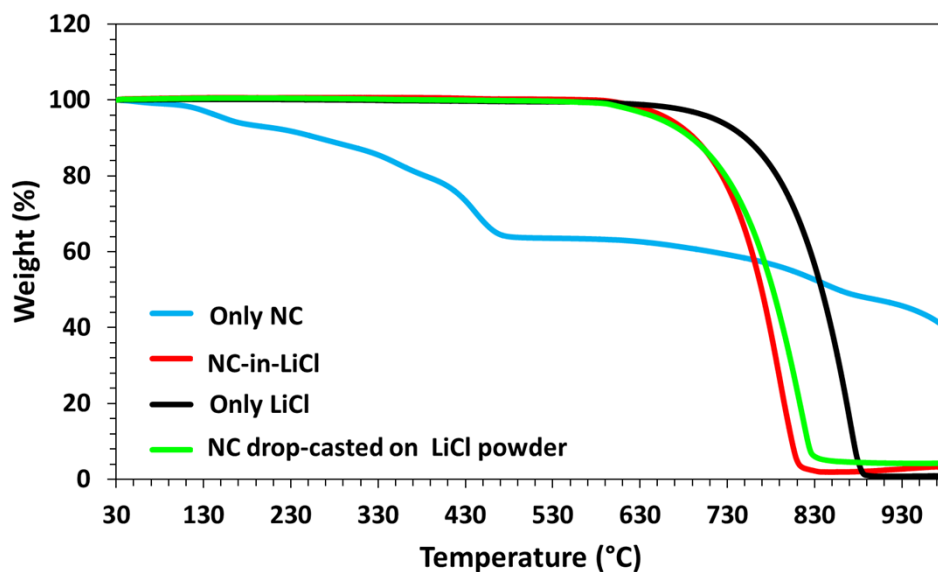


Figure S5. TGA curves of the NCs, NC-in-LiCl powders, only LiCl powders, and NC drop-casted on LiCl powders.

As seen from Figure S5, oleic acid capped-NCs have multiphase degradation with the increased temperature. Observed weight loss between 30-150 °C and 150-450 °C occurs due to the evaporation of hexane from the sample and degradation of oleic acid ligands⁶, respectively. On the other hand, only LiCl, NC-in-LiCl and NC drop-casted on LiCl samples have one-phase degradation and show a similar pattern. Above 600°C, linear mass loss was observed in LiCl including samples. It was attributed to the progressive vaporization of the salt LiCl near its melting point⁷. NC-in-LiCl powders exhibit faster weight loss compared to only LiCl powder. In order to understand whether chemical and physical interaction affects this difference, NC drop-casted on LiCl powder, in which we do not expect any chemical interaction, was also examined. We observed that NC drop-casting decreased the degradation temperature of the LiCl compared to only LiCl case, which was also the case for the NC-in-LiCl powders. In addition, NC drop-casted LiCl and NC-in-LiCl powders started to degrade at the same temperature and have almost the same temperature stability at the end. Therefore, we ascribed the stability difference between only LiCl powders and NC-in-LiCl powders mainly to physical effects. Furthermore, we did not observe a strong degradation phase in NC-in-LiCl or NC drop-casted on LiCl powders related to NCs, which is mainly due to low NC incorporation ratio into LiCl powders (~1%).

XPS measurements of the only NCs, NC-in-LiCl powders and only LiCl powders :

In order to study the interaction of the NCs with LiCl, we studied the XPS spectra of individual species and the mixture. XPS spectra are referenced to the C 1s peak at ~285 eV. For LiCl only

(Figure S5), in the Li spectra we observed two peaks which can be assigned to LiCl (56.33 eV) and Li₂O/Li₂CO₃ (55.24 eV), respectively. Similarly, in the Chlorine spectra (Figure S6) we observed the Cl 2p doublet (Cl 2p_{3/2} ~ 198.96 eV and Cl 2p_{1/2} ~ 200.7 eV) with an additional peak, which can be assigned to Cl-O/C-Cl (197.1 eV). This additional peak is most probably due to the moisture on LiCl. In the case of the NC-in-LiCl powders, XPS data do not show any new peak, which confirms the absence of any metal chloride (ZnCl₂ or CdCl₂) formation or interaction in the mixture. XPS spectra reveals a small shift (0.4 eV) in the Li and Cl peaks in the mixture (see Table S1), which is most probably due to the change in the medium. For the NCs (Figure S7), the XPS survey scan indicates the presence of Cd, Se, S and Zn. High resolution XPS spectra of all NC-elements are also obtained to study the interaction with the LiCl salt. For the NCs only, Cd 3d (Cd 3d_{5/2} ~ 405 eV and Cd 3d_{3/2} ~ 411.73 eV) and Zn 2p (Zn 2p_{3/2} ~ 1022.33 eV and Zn 2p_{1/2} ~ 1045.23 eV) doublet has been observed. Similarly, Se 3d (54.15 eV) and S 2p (162.04 eV) peaks are observed. For the mixture (Figure S6) we observe a small shift (0.5 eV) in the NC peaks in comparison to the only NC case (see Table S1), which is most probably due to the change in the microenvironment of the NCs. XPS results therefore support the notion that the NCs and LiCl form a composite structure and NC incorporation into LiCl is also confirmed by the decrease in the intensity of the NCs peaks in comparison to the only NCs, since XPS is a surface sensitive technique (Figure S7).

Table S1: XPS data for the only NCs, NC-in-LiCl, and only LiCl samples.

Element	Only LiCl (eV)	Only NCs (eV)	NC-in-LiCl (eV)	Difference (eV)
Li	56.33	-----	56.78	0.45
Cl	198.96	-----	199.35	0.39
Cd	-----	405	405.52	0.52
Zn	-----	1022.33	1022.84	0.51
Se	-----	54.15	-----	-----
S	-----	162.04	162.6	0.56

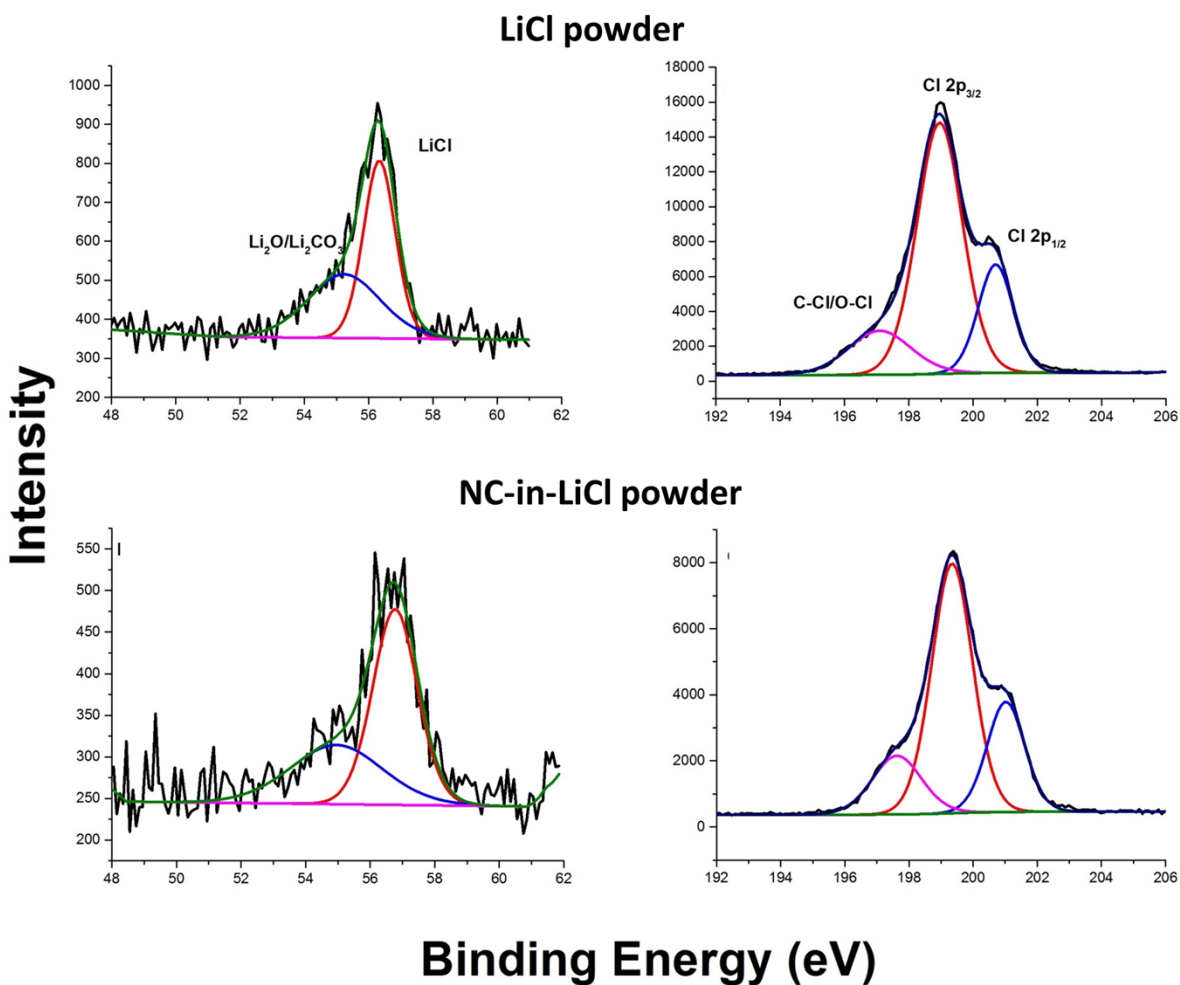


Figure S6. XPS spectra comparison of Li and Cl peaks in only LiCl and NC-in-LiCl samples.

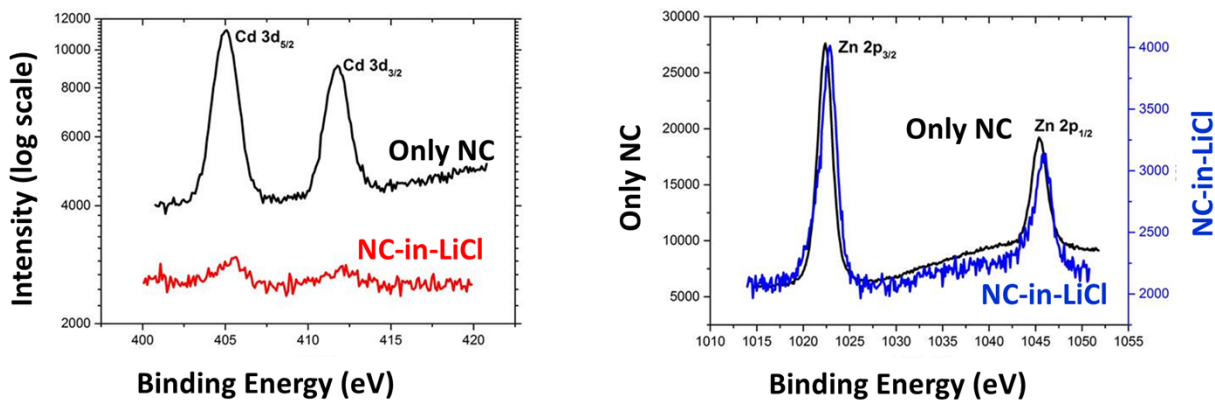


Figure S7. XPS spectra comparison of Zn and Cd peaks in the only NCs and NC-in-LiCl samples.

References:

- 1 G. Nienhuis, C. Th. J. Alkemade, *Physica B & C*, 1976, **81C**, 181.
- 2 R. J. Glauber, M. Lewenstein, *Phys. Rev. A*, 1991, **43**, 467.
- 3 J. Knoester, S. Mukamel, *Phys. Rev. A*, 1989, **40**, 7065.
- 4 M. E. Crenshaw, C. M. Bowden, *Phys. Rev. Lett.*, 2000, **85**, 1851.
- 5 Z. A. Talib, W. M. Daud, Y. N. Loh, H. A. A. Sidek, *Ionics*, 2008, **15**, 369-376.
- 6 A. Sarkar and S. Mahapatra, *J. Mater. Chem. A*, 2014, **2**, 3808-3818.
- 7 P. J. Masset, *J. Therm. Anal. Calorim.*, 2009, **2**, 439-441.